

Perfect quantum state transfer with spinor bosons on weighted graphs

David L. Feder

Department of Physics and Astronomy and Institute for Quantum Information Science,
University of Calgary, Calgary, Alberta, Canada T2N 1N4

(Dated: April 17, 2018)

A duality between the properties of many spinor bosons on a regular lattice and those of a single particle on a weighted graph reveals that a quantum particle can traverse an infinite hierarchy of networks with perfect probability in polynomial time, even as the number of nodes increases exponentially. The one-dimensional ‘quantum wire’ and the hypercube are special cases in this construction, where the number of spin degrees of freedom is equal to one and the number of particles, respectively. An implementation of near-perfect quantum state transfer across a weighted parallelepiped with ultracold atoms in optical lattices is discussed.

PACS numbers: 02.10.Ox,03.65.Ud,03.67.a,05.30.Jp

The quantum walk (QW) is the quantum mechanical extension of the classical random walk, where the quantum particle (the walker) can be thought of as following many trajectories simultaneously [1]. For quantum walks on regular (unweighted) linear graphs, the mean displacement of the particle is quadratically faster than that of a classical random walk [2]. The time needed to propagate from the input to the output vertex for certain two-dimensional regular graphs with randomization has been shown to be exponentially faster than with any classical algorithm [3], but like the linear graph the probability of hitting the output vertex decreases polynomially with the graph width. Perfect output probability can be achieved on the n -dimensional hypercube [4, 5] based on regular and weighted one-dimensional graphs [6] with an exponential speed-up over a classical random walk, though the improvement is only polynomial compared with a suitable classical algorithm [3].

Quantum walks on weighted graphs have been proposed as an efficient way to transfer quantum states (and therefore quantum information) with perfect fidelity without requiring external control [6]. To maximize throughput, it would be most convenient to transport many quantum states simultaneously. Unfortunately, the quantum particles on which the information is encoded are usually *indistinguishable*; if the receiver needs to know both the information and the particular carrier (where the latter might represent a given wire in a quantum circuit, for example), then the particles need to be spatially or temporally separated. For many applications it is sufficient to know only that a certain amount of information has been transmitted, however. For example, Alice might want to send Bob M copies of a given quantum state (entangled or otherwise), or one qudit each of M Bell pairs so that Alice and Bob can share M ebits, or $N - 1$ qudits of a GHZ _{N} or complete graph state, etc.

As discussed in detail below, many spinor bosons undergoing continuous-time quantum walks (CTQWs) can be mapped to a single particle walking on an infinite hierarchy of weighted graphs, including (but not limited

to) weighted hyperparallelepipeds, hypertetrahedra and hyperoctahedra. These graphs generally have vertices of variable degree, and share the property with the hypercubes that they can be traversed with unit probability in polynomial time. Unlike the hypercubes, however, there is no known classical algorithm that can accomplish the same task. The unique properties of walks on these graphs may aid in the development of new schemes for quantum communication and computation.

Consider N bosons with S spin (or pseudospin) degrees of freedom, located on a connected graph with V vertices of minimal degree one. The $(N_\sigma + V - 1)!/N_\sigma!/(V - 1)!$ accessible quantum states for each spin projection $\sigma \in \{-\frac{(S-1)}{2}, -\frac{(S-3)}{2}, \dots, \frac{(S-3)}{2}, \frac{(S-1)}{2}\}$ are defined by the Bose occupation of the various sites; that is, the natural basis states are defined in Fock (occupation number) space. Explicitly, for a two-site lattice the $\prod_\sigma (N_\sigma + 1)$ states are

$$|n_1, n_2\rangle = \prod_{\sigma\sigma'} \frac{1}{\sqrt{n_{1\sigma}! n_{2\sigma'}!}} \left(a_{1\sigma}^\dagger\right)^{n_{1\sigma}} \left(a_{2\sigma'}^\dagger\right)^{n_{2\sigma'}} |\mathbf{0}\rangle, \quad (1)$$

where the quantum numbers $n_{i\sigma} \in \{0, 1, 2, \dots, N\}$ denote the number of bosons with spin projection σ in the site i , $|\mathbf{0}\rangle$ denotes the particle vacuum, and $\sum_{i\sigma} n_{i\sigma} = N$. In this second-quantized notation, the operators $a_{i\sigma}^\dagger$ and $a_{i\sigma}$ create and annihilate, respectively, a boson with spin projection σ in site i . The normalization factors reflect the $n_{i\sigma}!$ ways that $n_{i\sigma}$ identical bosons can be arranged among themselves. Thus each basis state encodes the symmetric permutation of all quantum states with the same Hamming weight. The basis states for N bosons on V sites are obvious generalizations of these, requiring at most VS quantum numbers $n_{1\sigma}, n_{2\sigma}, \dots, n_{V\sigma}$.

The dynamics of this system are described by the hopping Hamiltonian:

$$H = \sum_{\langle ij \rangle \sigma} \tau_{ij} \hat{a}_{j\sigma}^\dagger \hat{a}_{i\sigma}, \quad (2)$$

where τ_{ij} is amplitude to hop between sites i and j , and the angle brackets denote a sum over only nearest neigh-

bors of a given vertex connected by an edge. The hopping amplitudes therefore define the adjacency matrix of the graph, which is assumed to be undirected ($\tau_{ij} = \tau_{ji}$) but otherwise unconstrained. The only non-zero matrix elements of the Hamiltonian (2) connect an N -particle Fock basis state to another where one boson with spin projection σ is annihilated at site i and another with the same spin is created in an adjacent site j . Consider, for example, the matrix element connecting the states $|n_1, n_2, n_3\rangle$ and $|n_1, n_2 - 1, n_3 + 1\rangle$, assuming all spin states are equal. Because each quantum number labels a different (site) subspace, the matrix element decomposes into a tensor product of matrix elements for the three sites. If the hopping amplitude between these states is τ one obtains:

$$\begin{aligned} & \langle n_1, n_2 - 1, n_3 + 1 | H | n_1, n_2, n_3 \rangle \\ &= \tau \frac{1}{n_1!} \langle 0 | \left(a_1 \right)^{n_1} \left(a_1^\dagger \right)^{n_1} | 0 \rangle \\ & \quad \otimes \frac{1}{\sqrt{(n_2 - 1)! n_2!}} \langle 0 | \left(a_2 \right)^{n_2 - 1} a_2 \left(a_2^\dagger \right)^{n_2} | 0 \rangle \\ & \quad \otimes \frac{1}{\sqrt{(n_3 + 1)! n_3!}} \langle 0 | \left(a_3 \right)^{n_3 + 1} a_3^\dagger \left(a_3^\dagger \right)^{n_3} | 0 \rangle \\ &= \tau \sqrt{\frac{n_2! (n_3 + 1)!}{(n_2 - 1)! n_3!}} = \tau \sqrt{n_2 (n_3 + 1)}. \end{aligned} \quad (3)$$

All other elements of the Hamiltonian can be obtained by suitably replacing any of the n_i .

The N -particle quantum walk on the original (primary) graph is therefore dual to a one-particle walk on a secondary graph whose vertices are labeled by the Fock states and whose adjacency matrix is defined by the Hamiltonian matrix elements above. Since the Hamiltonian is constant in time, the CTQW walk is effected by propagating the Fock-space wavefunction according to $|\psi(t)\rangle = U(t)|\psi(0)\rangle$ where the time-dependent unitary is $U(t) = e^{-iHt}$. Starting with unit probability on the input vertex, the CTQW is executed until the probability at the output vertex is maximized; this defines the hitting time t_h . The choice of input and output vertices depends on the structure of the graph, and will be clarified below.

Suppose that the primary graph P is the two-vertex chain, with the input and output vertices corresponding to left and right sites, respectively; this can be traversed with 100% probability with a CTQW in constant time $t_h = (\pi/2)\tau^{-1}$ [4]. This value of t_h is independent of N because each boson executes its own independent quantum walk on the primary graph. The original eigenvalues $\lambda = \{\pm\tau\}$ are transformed into the N -multiples $\lambda = \tau\{-N, -N + 2, \dots, N - 2, N\}$ which are always commensurate [6]. The resulting structure of the evolution operator $U(t)$ on the secondary graph ensures that perfect state transfer occurs between each pair of symmetry-related vertices at $t = t_h$, i.e. between any two vertices whose quantum numbers are related by inversion $|n_{1\sigma}, n_{2\sigma}, \dots, n_{V\sigma}\rangle \leftrightarrow |n_{V\sigma}, \dots, n_{2\sigma}, n_{1\sigma}\rangle$.

Choosing $N = S$ so that there are N distinguishable bosons, then $n_{i\sigma} \in \{0, 1\}$ for each value of σ and the matrix elements (3) are all equal to τ . As expected, the system maps to the N -dimensional τ -length hypercube $P^{\otimes N}$, which has the same value of t_h . When $S = 1$ so that all the bosons are spinless and therefore indistinguishable, the secondary graph G_N is the weighed line whose $N + 1$ vertices are labeled by the Fock states $|N - n, n\rangle$ where $n \in \{0, 1, \dots, N\}$ and the edge weights are given by $H_{n,n+1} = \tau \sqrt{(n+1)(N-n)}$. These are precisely the weights required to transport a quantum state across a quantum wire, also in time $t_h = (\pi/2)\tau^{-1}$ [6] which has been shown to be optimal [7]. In fact, as has been noted [4], these weights result from projecting the vertices of an N -dimensional unit-length hypercube onto a line. The boson construction indicates that the projection is driven by indistinguishability: all states of the hypercube with the same Hamming weight are mapped to a common point on the line, but the bit positions in the original strings are not specified.

Suppose that the N bosons each carry the qudit state $|\psi\rangle = c_1 | -\frac{(S-1)}{2} \rangle + \dots + c_S | \frac{(S-1)}{2} \rangle$, where $\sum_{i=1}^S |c_i|^2 = 1$. Because the Hamiltonian (2) preserves the total spin, the N -particle walk decomposes into a superposition of walks on S graphs of the type G_N (quantum wires), $S(S-1)$ graphs of type $G_{N-1} \otimes P$ (weighted rectangles), $S(S-1)(S-2)/2$ graphs of type $G_{N-2} \otimes P^{\otimes 2}$, $S(S-1)$ graphs of type $G_{N-2} \otimes G_2$, etc. These secondary graphs are hyperparallelepipeds of maximum dimension S , where along each direction the edge weights correspond to those of the quantum wire. Perfect quantum state transfer is effected between any two vertices connected by a line through the geometric center of the hyperparallelepiped.

Consider now N' bosons randomly distributed on one of the weighted secondary graphs. At $t = t_h$, the quantum state labeled by the Bose occupations for each site is transformed into another state with the same populations in the symmetry-related sites. This final quantum state corresponds to a site that is itself the symmetry counterpart to the initial site on a tertiary graph. In this manner one can generate an infinite hierarchy of weighted graphs that all share the properties of the primary graph. The largest edge weight is proportional to $N_m \cdots N_2 N_1$ where N_m is the number of bosons at recursion level m ; rescaling this weight back to τ yields a physical hitting time $t_h \propto \prod_{i=1}^m N_i$ that increases polynomially even as the number of vertices grows exponentially.

The smallest tertiary graphs built from quantum wires and hypercubes are shown in Fig. 1 for $S' = 1$. With N' indistinguishable bosons on G_N , the resulting graphs are N -dimensional weighted hypertetrahedra with $N' + 1$ vertices along each edge, but where not all vertices share an edge with their nearest neighbors. For the two-dimensional graphs defined by N' bosons on G_2 , shown in Figs. 1(a-c), the edges between V vertices along a given

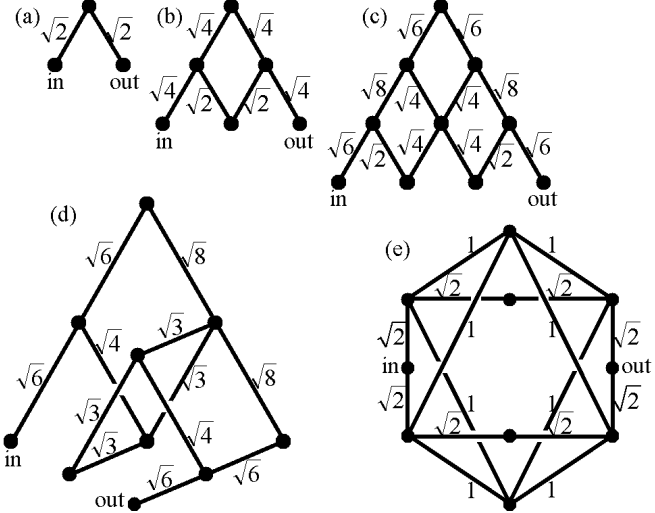


FIG. 1: Examples of small tertiary graphs built from the quantum wire and hypercube. Cases (a) through (c) correspond to $N = 1$ through 3 on G_2 ; cases (d) and (e) depict $N = 2$ on G_3 (tetrahedron of length 2) and on $P \otimes P$ (octahedron of base length 2), respectively. All weights are in units of τ . A CTQW running for $t = (\pi/2)\tau^{-1}$ will yield perfect quantum state transfer between vertices ‘in’ and ‘out’.

constant direction have weights defined by $V - 1$ bosons on P , multiplied by $\sqrt{2}$; perfect quantum transfer occurs between any two vertices related by a reflection about the graph center, so that states on central vertices remain fixed at intervals of t_h . N' bosons on the square \square (two-dimensional unweighted hypercube) map to a single boson on (generally truncated) octahedra with $N' + 1$ vertices along each edge of the square base, as shown in Fig. 1(e); quantum states are transferred to between vertices through the body center and parallel to the base, so that states on the two apices remain fixed at t_h intervals.

The edge weights on high-order graphs in this construction generally increase both with N' and the number of vertices, as is evident in Figs. 1(a)-(c). Consider for example the graphs defined by a hierarchy of spinless bosons $\{N_m \text{ on } [\dots N_1 \text{ on } (N_0 \text{ on } 2^{\otimes d})]\}$, where d is the secondary hypercube dimension and m is the number of iterations in the hierarchy used to construct the graph. Because of the symmetry of the underlying graphs at each level, edges with the largest weights are contiguous. This implies an efficient classical algorithm to traverse these graphs with high probability and relatively few steps: one simply chooses the ‘heaviest’ edges at each step.

Graphs avoiding this issue include constructions such as $\{N_m \text{ on } [\dots [N_1 \text{ on } (N_0 \text{ on } 2)]^{\otimes S_1} \dots]^{\otimes S_m}\}$, with N_1 distinguishable bosons on hypertetrahedra forming the underlying graph for N_2 distinguishable bosons, etc. An example is shown in Fig. 2. When these graphs get very large, the weights tend to become homogeneously distributed; because the vertex degrees also vary across the network, there are no identifiable criteria that can be

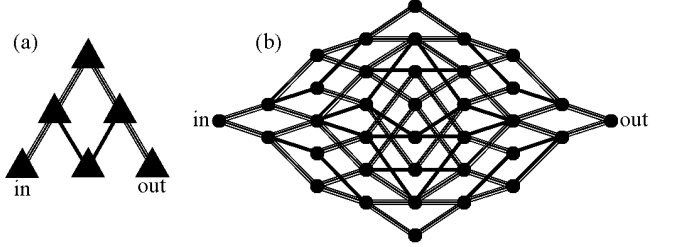


FIG. 2: Two representations of the same four-dimensional fourth-order graph $(2 \text{ on } G_2)^{\otimes 2} = [2 \text{ on } (2 \text{ on } 2)]^{\otimes 2}$. Each triangular node in (a) corresponds to the six-vertex weighted graph shown in Fig. 1(b); each node within a triangle connects to its counterpart in an adjacent triangle by an edge with the same weight. Solid and striped lines correspond to edges with weight $\sqrt{2}$ and $\sqrt{4}$, respectively.

used to classically determine the optimal edge at each step. Together with an exponential increase in the number of vertices, this implies an exponential speed-up of the quantum walk over any classical traversal algorithm.

The two-vertex graph need not be the only primary graph that yields perfect quantum state transfer, however, if the weights are allowed to be complex. The resulting hierarchy of higher-order graphs are the quantum analog of signed classical networks. In this case the hopping Hamiltonian becomes $H = \sum_{\langle ij \rangle \sigma} (\tau_{ij} \hat{a}_{j\sigma}^\dagger \hat{a}_{i\sigma} + \text{H.c.})$, where τ is now complex and ‘H.c.’ stands for ‘Hermitian conjugate.’ One of these is the triangle Δ with edge weights $i\tau/\sqrt{3}$ and eigenvalues $\lambda = \{\pm\tau, 0\}$. Labeling the vertices clockwise around Δ , the state is transferred to each successive neighbour in a counterclockwise fashion after each time interval $t = (2\pi/3)\tau^{-1}$. The secondary graphs generated with N bosons on Δ correspond to weighted triangles and tetrahedra. These are much like Figs. 1(a-c), in that the weights are defined by the G_V graph with $V + 1$ vertices along a given direction (multiplied by $i/\sqrt{3}$), except that all nearest neighbors now share an edge. Quantum states are successively transferred between vertices related by a counterclockwise $2\pi/3$ rotation about the center, which is a symmetry operation for the graph. Another example is the square \square or bowtie \bowtie with successive weights $1, e^{i\alpha}, e^{i\beta}, e^{i\gamma}$ in units of τ , where the first weight can be chosen to be real without loss of generality; $P \otimes P$ is a special case with $\alpha = \beta = \gamma = 0$. Whenever $\gamma = \alpha + \beta$, the eigenvalues are $\lambda = \{\pm\tau\}$ and perfect state transfer occurs between vertices at opposite corners.

That the eigenvalues of the hopping Hamiltonian on the primary graph are commensurate and symmetric about zero is a necessary but insufficient condition for perfect state transfer, however. For example, the complete four-vertex graph can have weights a on outside edges and weights b on the inside (diagonal) edges, while still preserving $\pi/4$ -rotation symmetry. For example, choosing $a = i/\sqrt{2}$ and $b = i$ yields $\lambda = \{\pm 2\tau, 0\}$ but

after $t_h = \pi/2\tau$ the state is in an equal superposition of two vertices. While it is conceivable that a judicious choice of weights could guarantee perfect state transfer between two nodes of an arbitrary graph, the prescription for accomplishing this has not been determined.

Ultracold atomic spinor bosons confined in optical lattices [8, 9, 10] provide a physical system that is particularly amenable to implementing perfect quantum state transfer on some of the weighted networks discussed above, especially those with regular geometries. The atomic interactions can be made small through the use of Feshbach resonances [11], and the tunneling amplitudes and phases from site to site can be controlled to some extent [12]. Particularly simple graphs to physically construct are the secondary weighted parallelepipeds $G_V^{\otimes d}$ where $1 \leq d \leq 3$ and the weighted tetrahedra based on Δ with complex weights. The tunneling matrix elements along any given direction now depend on position, $\tau_{i-1,i} = \tau\sqrt{i(V-i+1)}$ with $1 \leq i \leq V$. With the substitution $i = [(V+1)/2] - j$ where j is the vertex index relative to the graph center, one finds $\tau_{j-1,j}^2 \propto [(V+1)/2]^2 - j^2$. For standard optical lattice potentials of the form $\hat{V}(\tilde{x}) = sE_R \cos^2(k\tilde{x})$, where $\tilde{x} = \{x, y, z\}$, $k = 2\pi/\lambda$ is the wavevector (λ is the laser wavelength), and s is the lattice depth in units of the atomic recoil energy $E_R = \hbar^2 k^2 / 2m$ (m is the atomic mass), the tight-binding approximation applicable for $s \gtrsim 5$ gives $\tau^2 = (16/\pi)s^{3/2}e^{-4\sqrt{s}}$ in recoil energies [13]. The required quadratic variation of $\tau_{j-1,j}^2$ can be approximately obtained by choosing a weak position-dependent lattice depth $s = s_0 + aj^2$ in each direction, which in principle can be accomplished by appropriately focusing the lattice laser beam and adding end caps to provide hard-wall boundary conditions.

The Schrödinger equation for bosons in a one-dimensional (1D) optical lattice with $V = 101$ and $s_0 = 5$ was propagated in time numerically using a finite-element discrete variable approach [14]. Choosing $a = 10^{-3}$ and $S = 1$, an initial quantum state centered at $j_0 = \{10, 20, 30, 40\}$ and spread over several sites was found to transfer to the sites located symmetrically opposite the lattice center with probabilities exceeding 99%. The hitting times were within 10% of the theoretical value $t_h = (V+1)(\pi^{3/2}/16)s^{-3/4}e^{2\sqrt{s}}(\hbar/E_R) \approx 40$ ms, assuming ^{87}Rb atoms in a lattice with $\lambda = 800$ nm. Surprisingly, the initial wavepacket remains well-localized during the propagation. Weak damping of the oscillations between initial and final states is due to increased dispersion driven by the imperfect phase profile (which is more pronounced near the lattice edge), and was found to have a characteristic time between $42t_h$ ($j_0 = 40$) and $116t_h$ ($j_0 = 10$).

Precise control of the lattice potential or atomic interactions is not required to effect the state transfer. For example, choosing $a = 7 \cdot 10^{-3}$ when $V = 101$ gives a variation of the hopping amplitudes that is more appro-

priate for a lattice with $V = 41$. State transfer with probability exceeding 95% was found for any $j_0 \leq 20$ within approximately 10% of $t_h = 380\tau^{-1}$. For $j_0 > 20$, the wavepacket remained at the lattice periphery. Virtually identical behavior was obtained using a Gaussian, rather than quadratic, profile for the lattice height. Weak repulsive interactions between bosons were incorporated in a mean-field sense by solving the appropriate quasi-1D nonlinear Schrödinger equation. The strength of the additional term $g|\psi|^2$ is parametrized by the effective 1D interaction strength g , which in the current dimensionless units is $g = a_s\lambda/\pi^2\ell_\perp$ [15] where a_s is the s -wave scattering length and ℓ_\perp is the transverse oscillator length. For parameters relevant to current experiments [10], $g \approx 0.2$. For values of $g \leq 1$, t_h is found numerically to increase only slightly (by 3%), and the probability of hitting the output vertex decreases to 95%. Because the t_h are identical for all sites, the behavior for this range of interaction strengths is only weakly dependent on the initial density distribution. For larger values of g the output probability drops precipitously, but the mean-field approximation becomes increasingly suspect. The numerical results suggest that near-perfect quantum state transfer can be achieved using ultracold bosons in weighted optical lattices under realistic experimental conditions.

It is a pleasure to thank Peter Hoyer and John Watrous for stimulating conversations. This work was supported in part by the Natural Sciences and Engineering Research Council of Canada and the Canada Foundation for Innovation.

-
- [1] J. Kempe, *Contemporary Physics* **44** 307 (2003); A. Ambainis, *Int. J. Quantum Inf.* **1**, 507 (2003).
 - [2] D. Aharonov, A. Ambainis, J. Kempe, and U. Vazirani, *Proceedings of ACM Symposium on the Theory of Computation*, 50 (2001).
 - [3] A. M. Childs, E. Farhi, and S. Gutmann, *Quantum Inf. Proc.* **1**, 35 (2002).
 - [4] N. Shenvi, J. Kempe, and K. B. Whaley, *Phys. Rev. A* **67**, 052307 (2003).
 - [5] J. Kempe, *Probability Theory and Related Fields* **133**, 215 (2005).
 - [6] M. Christandl, N. Datta, A. Ekert, and A. J. Landahl, *Phys. Rev. Lett.* **92**, 187902 (2004); M. Christandl *et al.*, *Phys. Rev. A* **71**, 032312 (2005).
 - [7] M.-H. Yung, [quant-ph/0603179](#).
 - [8] T. Stöferle *et al.*, *Phys. Rev. Lett.* **92**, 130403 (2004).
 - [9] B. Paredes *et al.*, *Nature* **429**, 277-281 (2004).
 - [10] C. D. Fertig *et al.*, *Phys. Rev. Lett.* **94**, 120403 (2005).
 - [11] S. L. Cornish *et al.*, *Phys. Rev. Lett.* **85**, 1795 (2000).
 - [12] E. J. Mueller, *Phys. Rev. A* **70**, 041603(R) (2004).
 - [13] G. Pupillo, C. J. Williams, and N. V. Prokof'ev, *Phys. Rev. A* **73**, 013408 (2006).
 - [14] B. I. Schneider, L. A. Collins, and S. X. Hu, *Phys. Rev. E* **73**, 036708 (2006).
 - [15] M. Olshanii, *Phys. Rev. Lett.* **81**, 938 (1998).